Journal of
Synchrotron Radiation

ISSN 0909-0495

Received 15 October 2005
Accepted 20 December 2005

A cryogenically stabilized meV-monochromator for hard X-rays

T. S. Toellner,* A. Alatas, A. Said, D. Shu, W. Sturhahn and J. Zhao

Advanced Photon Source, Argonne National Laboratory, Argonne, IL 60439, USA.
E-mail: toellner@anl.gov

The design and performance results for a cryogenically stabilized high-resolution monochromator for 23.880 keV (λ = 52 pm) X-rays are presented. The four-crystal-reflection monochromator is suitable for nuclear resonant scattering measurements from ^{119}Sn compounds using synchrotron radiation. The design includes a low-vibration cryostat that maintains two of the four crystal reflections at a temperature where the coefficient for thermal expansion of the crystalline material (silicon) vanishes. Test results demonstrate a 1.3 meV bandwidth with negligible broadening due to vibrations and a spectral efficiency of 37% when used with an undulator source.

Keywords: high resolution; monochromator; X-rays; cryostat; Sn.

1. Introduction

High-resolution monochromatization has important spectroscopic and metrological applications. In the 1 Å-wavelength region, applications include inelastic X-ray scattering (Burkel, 1991), nuclear resonant scattering (Gerdau & de Waard, 1999) and precise wavelength measurements (Shvyd'ko *et al.*, 2000). Metrological applications, like lattice-constant or wavelength determination, require high resolving power along with wavelength stability. Inelastic X-ray scattering is used to measure the microscopic dynamical behavior of solids and liquids. Owing to the desire to explore low-energy excitations and the weakness of the scattering, this technique requires monochromatization to the meV level with very high efficiency. Nuclear resonant scattering is used to measure the local chemical and dynamical behavior of nuclear resonant isotopes in a variety of materials. Because nuclear resonances in this wavelength region are extremely narrow ($\Delta E \simeq 10^{-8}$ eV), substantial monochromatization needs to be performed in a manner that preserves the available spectral flux. All of these high-resolution scattering techniques require narrow-bandwidth monochromatization of hard X-rays and directly benefit from improvements in efficiency and wavelength stability.

High-resolution monochromatization ($E/\Delta E > 10^6$) of synchrotron radiation in this wavelength region is typically performed either by using a near-back Bragg reflection from a crystal ($\Theta_B \simeq 90^\circ$) (Sette *et al.*, 1995) or by using a series of Bragg reflections ($\Theta_B < 90^\circ$) from a set of crystals (Toellner, 2000). The application determines the choice of one method over another. Near-back Bragg reflections have the advantage of large angular acceptances and are clearly favored when the radiation to be monochromated has a large divergence. For applications that restrict the energy, like nuclear resonant scattering, a near-back Bragg reflection is often not an option. This is due to the improbable energy match between the nuclear resonance energy and any of the limited number of back reflections that are available in crystalline materials of sufficient quality. Multiple-Bragg-diffracting arrangements have the advantage of allowing one to design a high-resolution monochromator (HRM) for a given energy and with a specified bandwidth. A design of such an HRM includes a physical arrangement of crystals, a judicious choice of crystal reflections, and the specification of their surface asymmetry angles. All this is done with the aim of maximizing efficiency. Despite the additional design effort, multiple-Bragg-diffracting monochromators offer substantial flexibility in terms of choice of energy, bandwidth, tunability range, exit geometry *etc.* Furthermore, multiple-Bragg-diffracting monochromators have demonstrated greater resolution (Toellner *et al.*, 2001; Yabashi *et al.*, 2001) and provide improved spectral response through greater suppression of components outside the nominal bandwidth.

There are a number of ways to improve the efficiency of high-resolution multiple-Bragg-diffracting monochromators. Apart from altering the incident beam properties, like reducing the vertical divergence that an HRM has to accept (Baron *et al.*, 1999), there are intrinsic aspects of a design that may be considered. These involve using crystal reflections that have high Debye–Waller factors. This can be done in three ways: using a crystalline material with a high Debye temperature, using only low-order crystal reflections, or lowering the temperature of the crystalline material. Owing to the resolutions and crystal diffraction volumes involved, it is important to use high-quality crystalline material that can be synthesized as large single crystals. For this reason, crystalline silicon is currently the most favored choice, even though other crystalline materials possess higher Debye temperatures and

therefore would provide larger Debye–Waller factors. Using only low-order crystal reflections as components of an HRM has the drawback of requiring a concomitant increase in the angular resolution needed to control the crystals. The required levels of vibration mitigation and angular step size quickly approach 1 nrad. The third way to increase Debye–Waller factors involves lowering the temperature of the crystalline material and has the complication of doing so while maintaining angular control of the crystal component on the level of a few tens of nanoradians. Despite suggestions of the many advantages of cryogenic stabilization of crystal components of HRMs (Toellner, 2000), vibration mitigation has been considered problematic and a barrier to its implementation. Here we demonstrate the viability of this method of improving efficiency by presenting a solution that achieves the requisite cooling with acceptable vibration levels.

Improvements in synchrotron radiation sources that lead to greater spectral flux can have a positive impact on high-resolution X-ray spectroscopies. With the production of greater spectral flux will come greater X-ray power loads in even pre-monochromated X-ray beams. At current third-generation synchrotron sources, in the X-ray energy range 20–30 keV, the X-ray power in pre-monochromated ($E/\Delta E \simeq 10^4$) X-ray beams is a few tens of milliwatts. Currently, some HRM designs already show degraded performance at these X-ray power loads (Toellner *et al.*, 2006). Also, HRM for higher energies and higher resolutions exhibit thermal sensitivity even to thermal gradients of their surrounding air. Cryogenic stabilization of HRMs at the zero-thermal-expansion-coefficient temperature of the crystalline material can mitigate a non-ideal performance by reducing the thermal sensitivity to the surrounding air as well as to increased X-ray power loads. In the case of silicon, the thermal-expansion coefficient vanishes at approximately 123 K and asymptotically below approximately 30 K (Touloukian *et al.*, 1977). Owing to the additional complexity of low-vibration cryogenics below 30 K, we designed an HRM that incorporates cryogenic stabilization at 123 K.

2. Design

We designed a multiple-Bragg-diffracting HRM for the 23.880 keV nuclear resonance in ^{119}Sn. This allows both a useful instrument for nuclear resonant scattering measurements on Sn-containing compounds as well as a practical means to characterizing the performance of the cryogenically stabilized HRM. The HRM is composed of two pairs of silicon lattice reflections arranged in a nested configuration (Ishikawa *et al.*, 1992). The outer pair of reflections are silicon (4 4 0) with a surface asymmetry angle of $\pm 14.5^\circ$ (asymmetry parameters $b_4 = b_1^{-1} = 24.3$), a Bragg angle of 15.7° and a size of 60 mm × 25 mm × 25 mm. The inner pair of reflections are silicon (12 12 12) with a surface asymmetry angle of $\pm 60.4^\circ$ (asymmetry parameters $b_2 = b_3^{-1} = 1.5$), a Bragg angle of 83.6° and a diffracting-surface size of 27 mm × 20 mm. These two pairs of crystal reflections are arranged as shown in Fig. 1. The HRM accepts 12.2 μrad (vertical) and 0.5 mm (vertical) of the incident X-ray beam. To reduce the number of motions necessary for energy scanning of the HRM, and because a 'channel-cut' crystal is not practical owing to its size, the outer crystals are designed as part of a weak-link assembly that allows both crystals to be rotated simultaneously with one rotation stage (Shu *et al.*, 2001; Toellner *et al.*, 2006). The introduction of a weak link into the design of the outer crystal pair allows the crystals to be fabricated separately and yet precisely aligned with respect to each other. Also, differences in crystal lattice spacing owing to thermal loading from the surrounding air or from the X-ray beam can be compensated for by a piezo actuator that is mounted on a lever arm linked to one of the crystals. The monochromatic X-ray divergence after the first crystal reflection is 0.5 μrad and the weak-link assembly allows the two outer crystals to be aligned with a precision of approximately 0.01 μrad. The inner pair of crystal reflections are the inside faces of a 'channel-cut' crystal, thus also allowing both reflections to be scanned together. At the cryogenic operating temperature, the angular acceptance of this 'channel-cut' crystal for monochromatic X-rays is 0.47 μrad, while the X-ray beam divergence between the two asymmetric faces is 0.7 μrad. The normals to the diffracting surfaces of the inner channel-cut crystal correspond to the $\pm(3\,7\,\bar{3})$ direction. This gives the mentioned asymmetry angle as well as constraining the diffraction plane to lie in a crystallographic zone relatively free of additional crystal reflections. All crystals are etched and all diffracting surfaces are polished. The inner and outer crystal pairs are mounted on concentric, but opposing, rotation stages.

The silicon (12 12 12) channel-cut crystal is cooled to 123 K. Assuming a Debye temperature of 530 K, this increases the Debye–Waller factor to 0.39 from a room-temperature value of 0.18. Owing to the relatively high room-temperature Debye–Waller factor of 0.88 for the silicon (4 4 0) reflection at 23.880 keV, and because the X-ray power load on the HRM is only 15 mW, there is little to be gained from the additional complexity of cooling the outer pair of reflections. Conse-

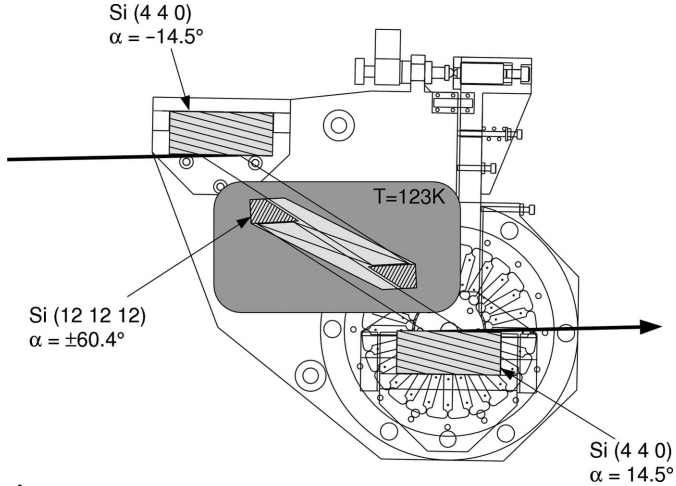

Figure 1
Design of the cryogenically stabilized high-resolution monochromator. The second and third crystal reflections are two faces of a monolithic crystal and are maintained at 123 K.

quently, the silicon (4 4 0) crystal reflections are maintained at room temperature. Owing to the sensitivity of the transmitted wavelength to the thermal expansion/contraction of the crystalline material, temperature monitoring of the room-temperature crystals is necessary. Calibrated thermistors are attached approximately 1 cm from the diffraction region on the silicon (4 4 0) reflections. For cryostat operation, the temperature of the silicon (12 12 12) crystal is monitored with two calibrated platinum resistors attached approximately 1 cm from each diffraction region.

The tunability range of the HRM is approximately 50 eV, the primary limitation being the physical shape of the asymmetrically cut inner channel-cut crystal. The calculated transmission function for σ-polarized photons as a function of energy and vertical angle of the incident beam is given in Fig. 2.

To cool the silicon (12 12 12) channel-cut crystal to 123 K, we constructed a low-vibration gas-flow cryostat. Cryogenically cooling an X-ray component that requires angular control to a few tens of nanoradians places a number of constraints on any practical design of a cryostat. First, the silicon channel-cut crystal needs to be rigidly coupled to a high-resolution rotation stage to allow the required motions to be executed. Second, the cooling must be performed in a manner that does not induce mechanical vibrations and does not deform the crystal. We designed a compact cryostat that satisfies these requirements, supports a large crystal (12 cm $\times$ 2 cm $\times$ 4 cm), and can be mounted directly onto a rotation stage (Kohzu KTG-15 with 25 nrad step^{-1}). Fig. 3 depicts the essential features of this design.

The design consists of a vacuum-jacketed sealed copper cryobox to hold the channel-cut crystal. The cryobox is cooled to approximately 123 K by circulating cold helium gas through channels in its base. The crystal is held in place within the cryobox using spring-loaded clamps, but is separated from the cryobox interior surfaces with thermal insulating shims. A helium exchange gas is used to achieve good thermal contact between the cryobox and the crystal without introducing mechanical stress. A rigid coupling between the cryobox and the mounting plate is effected by the use of a kinematic mounting system that uses three low-thermally conducting glass-epoxy posts. A low vibrational load is achieved by using two long (1.5 m) doubled-walled flexible transfer lines that transport the cooling gas and also provide a vacuum pathway for the vacuum jacket that surrounds the cryobox. Thus, the transfer lines and cryostat share the same insulating vacuum. The high-resolution rotation stage that supports the cryostat has load/moment limits that are adhered to by using an almost all-aluminium construction for the outer vacuum shroud. Beryllium windows (0.25 mm thick) are used on both the cryobox and vacuum shroud for transmission of the 23.880 keV X-ray beam. We monitored the temperature of the helium cooling gas at the inlet and outlet of the cryobox with the use of calibrated platinum resistors.

3. Testing

We measured the performance of the HRM at the 3-ID undulator beamline of the Advanced Photon Source. Synchrotron radiation produced from the two undulators (2.0 m and 2.5 m long) of this beamline passed through a water-cooled beryllium compound-refracting lens (CRL) before being monochromated at 23.880 keV using a water-cooled diamond (1 1 1) double-crystal pre-monochromator. The CRL produces a partial vertical collimation of the raw synchrotron radiation to bring the angular divergence of the X-rays into the narrow angular acceptance of the diamond (1 1 1) pre-monochromator (Zhao *et al.*, 2002). After the pre-

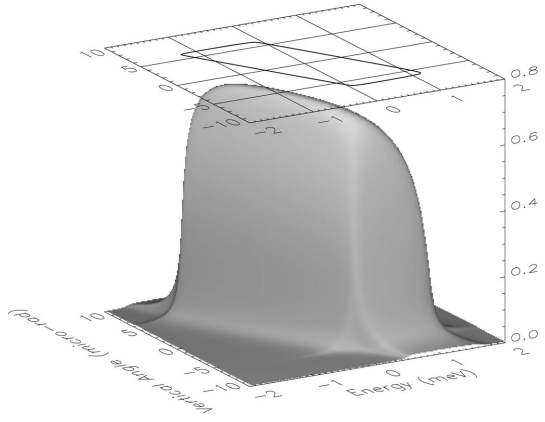

Figure 2
Calculated transmission function of HRM for 23.880 keV σ-polarized photons. The contour is drawn at 50% of peak transmission.

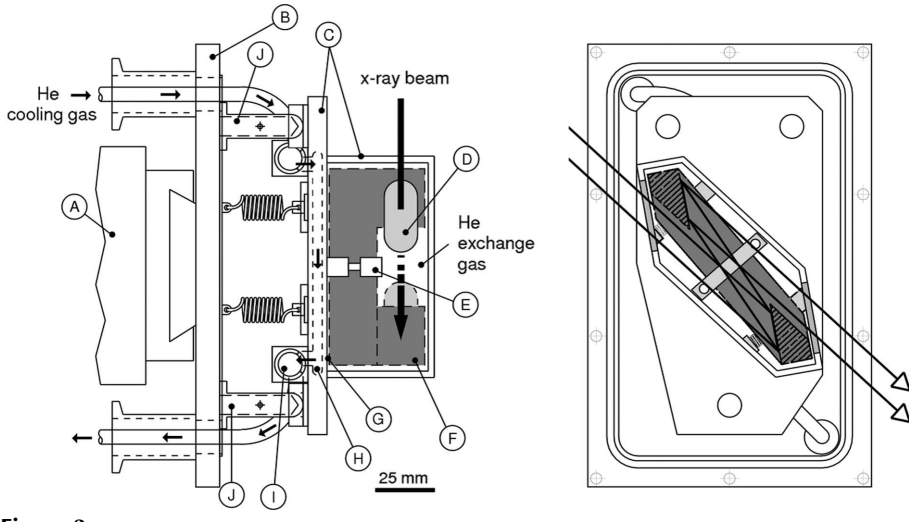

Figure 3
Cryostat used for cooling a silicon (12 12 12) channel-cut crystal to 123 K; high-resolution rotation stage (A), aluminium base plate (B), copper cryobox (C), beryllium windows (D), spring-loaded clamp (E), silicon crystal (F), thermal insulating shim (G), cooling channels (H), cooling-gas temperature sensors (I), glass-epoxy support post (J). Outer vacuum shroud and electrical feedthroughs are not shown.

monochromator, the energy bandwidth of the photon beam was 1.9 eV full width at-half maximum (FWHM). The HRM is placed after the pre-monochromator in such a way that the first crystal reflection is in a (+,+) scattering geometry with respect to the second crystal of the pre-monochromator. This provides approximately constant spectral transmission after the first reflection of the HRM over an energy range of a few hundred meV so that energy scan ranges that are less than approximately 200 meV may be performed by scanning the silicon (12 12 12) crystal pair only. The angle-to-energy conversion for the silicon (12 12 12) crystal pair is 0.384 μrad meV^{-1} plus twice the angular change of the outer pair of crystals if they are rotated. The angle-to-energy conversion for the outer silicon (4 4 0) crystal pair is 0.012 μrad meV^{-1}.

Characterization of the HRM performance involved a measurement of its energy-resolution function and its spectral efficiency. The energy-resolution function was measured by energy scanning the HRM through the 23.880 keV nuclear resonance of ^{119}Sn (in the form of $^{119}SnO/^{119}SnO_2$ powder) while monitoring the nuclear resonant flux that is scattered in the forward direction. Owing to the long lifetime of the nuclear resonance (τ = 26.4 ns), the nuclear resonant photons are delayed relative to the non-resonant photons and can be readily distinguished from the non-resonant scattering events with an avalanche photodiode detector and time-filtering electronics (Mooney *et al.*, 1994). This measurement produces the resolution function of the monochromator because of the δ-function-like energy response of the nuclear resonance in this scattering geometry. Both the measured result and the simulation are displayed in Fig. 4 and show excellent agreement. The energy bandwidth of the monochromator is 1.3 meV FWHM. This corresponds to a resolution ($E/\Delta E$) of 2×10^7.

In addition to the resolution function, the spectral efficiency can be measured and compared with a calculable result. An incident pre-monochromated X-ray beam of approximately 4.0×10^{12} photons s^{-1} in a 1.9 eV FWHM bandwidth, or a spectral flux of 2.1×10^{12} photons s^{-1} eV^{-1}, was reduced to an X-ray beam of 1.0×10^9 photons s^{-1} in a 1.3 meV FWHM bandwidth, or a spectral flux of 0.77×10^{12} photons s^{-1} eV^{-1}. We define the spectral efficiency as the ratio of the spectral flux after the HRM to the available spectral flux before the HRM (using the full pre-monochromated beam). Using this definition we obtain a measured spectral efficiency of 37%. This compares favorably with the theoretically expected result of 43%.

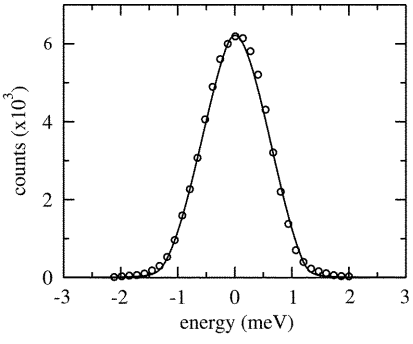

Figure 4
Resolution function of HRM measured with coherent resonant elastic scattering from the 23.880 keV nuclear resonance from ^{119}Sn. The solid line is the expected result. The energy width is 1.3 meV (FWHM).

4. Discussion

The cryogenically stabilized HRM produced a significant increase in spectral efficiency over a similarly designed room-temperature HRM. A similarly designed room-temperature four-crystal nested HRM for 23.880 keV X-rays that produces approximately a 1 meV energy bandwidth has a theoretical spectral efficiency of approximately 23% for the current X-ray source characteristics. In practice though, such a room-temperature version achieves a measured spectral efficiency of only 9% (Toellner *et al.*, 2006). The degraded performance is typical for room-temperature designs in this energy region and is due to thermally induced *d*-spacing variations over multi-reflecting monolithic crystals. Thus, the low-vibration cryostat mitigated the usual detrimental thermal effects present at room temperature as well as improving the intrinsic efficiency of the optic by 60%. Overall, the cryogenically stabilized HRM produced more than a factor of four increase in spectral efficiency over the room-temperature design.

The current design works well for existing X-ray power loads. Based on a 4.2 K temperature difference in the He cooling gas between the inlet and outlet of the cryobox, and a flow rate of 13 l min^{-1}, the cooling power was 0.8 W. Greater cooling power requirements, owing to increased X-ray power loads, would demand greater flow rates and potentially compromise the vibrational stability of the cryostat. Thus, one would expect this cryostat design to work for X-ray power loads that are small compared with 0.8 W, because flow rates would not have to increase substantially.

Vibrational loading from the off-axis transfer-line ports did not affect the angular reproducibility of the crystal during energy scans. In principle, it would be preferable to design the transfer-line ports to be coaxial with the rotation axis of the high-resolution rotation stage, as this would reduce the impact of any transfer-line-induced torque on the cryostat. This was not done, because such a design is not compatible with our rotation stage. The lack of any measurable consequence of transfer-line-induced torques is in part due to the limited angular range accessed with the cryostat. Applications involving the monochromator require maximum angular motions of less than 200 μrad, and no disruption of motion is noticeable within this range. Serendipitously, vibrational stability requirements are least where Θ_B is large. Thus, large-Bragg-angle crystal reflections, which experience the greatest increase in efficiency by cooling, are also the least sensitive to vibrations.

The current cryostat design is not limited to components of multiple-Bragg-diffracting HRMs. Other X-ray optics that would benefit from operating at cryogenic temperatures could also take advantage of this design, *e.g.* X-ray interferometers and meV analyzers. Applying cryogenics to near-back Bragg

reflections would improve their efficiency and their wavelength stability, but there are certain limitations with regard to energy tunability. Energy scanning a near-back Bragg reflection is performed by changing crystal temperature and relies on a non-vanishing thermal expansion coefficient. Consequently, if energy tunability is a requirement, then cryogenic stabilization of a near-back Bragg reflection must be performed at a temperature where the thermal expansion coefficient is non-zero. In contrast, energy scans for multiple-Bragg-diffracting monochromators are performed by changing crystal diffraction angles and can be tuned in energy even when the thermal expansion coefficient vanishes. A common application of near-back Bragg reflections is as large-angular-acceptance energy analyzers for inelastic X-ray scattering measurements. If such analyzers are used in combination with a multiple-Bragg-diffracting HRM, then they no longer require energy tunability, and their efficiency and thermal stability can be substantially improved with the use of cryogenics.

Use of the Advanced Photon Source was supported by the US Department of Energy, Office of Basic Energy Sciences, Office of Science under Contract W-31-109-ENG-38.

References

Baron, A. Q. R., Kohmura, Y., Ohishi, Y. & Ishikawa, T. (1999). *Appl. Phys. Lett.* **74**, 1492–1494.

Burkel, E. (1991). *Inelastic Scattering of X-rays with Very High Energy Resolution.* New York: Springer Verlag.

Gerdau, E. & de Waard, H. (1999). Editors. *Nuclear Resonant Scattering of Synchrotron Radiation.* The Netherlands: Baltzer Science.

Ishikawa, T., Yoda, Y., Izumi, K., Suzuki, C. K., Zhang, X. W., Ando, M. & Kikuta, S. (1992). *Rev. Sci. Instrum.* **63**, 1015–1018.

Mooney, T. M., Toellner, T. S., Sturhahn, W., Alp, E. E. & Shastri, S. D. (1994). *Nucl. Instrum. Methods A*, **347**, 348–351.

Sette, F., Ruocco, G., Krisch, M., Bergmann, U., Masciovecchio, C., Mazzacurati, V., Signorelli, G. & Verbeni, R. (1995). *Phys. Rev. Lett.* **75**, 850–853.

Shu, D., Toellner, T. S. & Alp, E. E. (2001). *Nucl. Instrum. Methods A*, **467–468**, 771–774.

Shvyd'ko, Y., Lerche, M., Jäschke, J., Lucht, M., Gerdau, E., Gerken, M., Rüter, H. D., Wille, H.-C., Becker, P., Alp, E. E., Sturhahn, W., Sutter, J. & Toellner, T. S. (2000). *Phys. Rev. Lett.* **85**, 495–498.

Toellner, T. S. (2000). *Hyperfine Interact.* **125**, 3–28.

Toellner, T. S., Hu, M. Y., Bortel, G., Sturhahn, W. & Shu, D. (2006). *Nucl. Instrum. Methods A*. In the press.

Toellner, T. S., Hu, M. Y., Sturhahn, W., Bortel, G., Alp, E. E. & Zhao, J. (2001). *J. Synchrotron Rad.* **8**, 1082–1086.

Touloukian, Y. S., Kirby, R. K., Taylor, R. E. & Lee, T. Y. R. (1977). *Thermophysical Properties of Matter*, Vol. 13, *Thermal Expansion – Nonmetallic Solids*, p. 154. New York: IFI/Plenum Press.

Yabashi, M., Tamasaku, K., Kikuta, S. & Ishikawa, T. (2001). *Rev. Sci. Instrum.* **72**, 4080–4083.

Zhao, J. Y., Alp, E. E., Toellner, T. S., Sturhahn, W., Sinn, H. & Shu, D. (2002). *Rev. Sci. Instrum.* **73**, 1611–1613.